

Solar Abundances of Rock Forming Elements, Extreme Oxygen and Hydrogen in a Young Polluted White Dwarf

J. Farihi^{1*}†, D. Koester², B. Zuckerman³, L. Vican³, B. T. Gänsicke⁴, N. Smith⁵,
G. Walth⁵, E. Breed⁴

¹Department of Physics and Astronomy, University College London, London WC1E 6BT

²Institut für Theoretische Physik und Astrophysik, University of Kiel, 24098 Kiel, Germany

³Department of Physics and Astronomy, University of California, Los Angeles CA 90095, USA

⁴Department of Physics, University of Warwick, Coventry CV4 7AL

⁵Steward Observatory, University of Arizona, Tucson AZ 85721, USA

ABSTRACT

The $T_{\text{eff}} = 20800$ K white dwarf WD 1536+520 is shown to have broadly solar abundances of the major rock forming elements O, Mg, Al, Si, Ca, and Fe, together with a strong relative depletion in the volatile elements C and S. In addition to the highest metal abundances observed to date, including $\log(\text{O}/\text{He}) = -3.4$, the helium-dominated atmosphere has an exceptional hydrogen abundance at $\log(\text{H}/\text{He}) = -1.7$. Within the uncertainties, the metal-to-metal ratios are consistent with the accretion of an H_2O -rich and rocky parent body, an interpretation supported by the anomalously high trace hydrogen. The mixed atmosphere yields unusually short diffusion timescales for a helium atmosphere white dwarf, of no more than a few hundred yr, and equivalent to those in a much cooler, hydrogen-rich star. The overall heavy element abundances of the disrupted parent body deviate modestly from a bulk Earth pattern, and suggest the deposition of some core-like material. The total inferred accretion rate is $4.2 \times 10^9 \text{ g s}^{-1}$, and at least 4 times higher than any white dwarf with a comparable diffusion timescale. Notably, when accretion is exhausted in this system, both metals and hydrogen will become undetectable within roughly 300 Myr, thus supporting a scenario where the trace hydrogen is related to the ongoing accretion of planetary debris.

Key words: circumstellar matter— stars: abundances— stars: individual (WD 1536+520)— planetary systems— white dwarfs

1 INTRODUCTION

A decade of observational and theoretical studies by many astronomers has shown that, over a wide range of effective stellar temperatures, the presence of heavy elements in white dwarf atmospheres is evidence for orbiting planetary systems (Farihi 2016; Vanderburg et al. 2015; Jura & Young 2014; Veras et al. 2015). With this relatively recent shift in paradigm, the discovery of the prototype, metal-lined white dwarf by van Maanen (1917) nearly a century ago – while not a planet detection itself, but the signature of accreted planetary debris – is arguably the first astronomical evidence of the presence of planetary systems around other stars (Zuckerman 2015).

According to all dynamical models that deliver sufficient planetesimal masses into the innermost system where it can be accreted, each exoplanetary system hosted by a metal-enriched white dwarf must harbor at least a belt of minor bodies and one ma-

jor planet (Frewen & Hansen 2014; Veras et al. 2013; Debes et al. 2012; Bonsor et al. 2011). The gravitational field of the planet(s) can perturb the orbits of the planetesimals onto orbits passing near the white dwarf so that they are tidally disrupted. *Spitzer* and complementary ground-based observations have established a firm connection between the atmospheric heavy elements in white dwarfs and the presence of dust and gas within the tidal radius of the star (Farihi et al. 2009; von Hippel et al. 2007; Jura et al. 2007; Gänsicke et al. 2006).

Because the metal-to-metal sinking timescales vary by no more than a factor of a few, the relative, steady-state abundances of the accreted planetary debris can be analytically linked to those observed in the polluted atmosphere (Koester 2009), thus making the stellar surface an effective mirror of planetesimal composition. The first detailed abundance study of any metal-enriched white dwarf was carried out for the current record holder for number (16) of detected heavy elements, GD 362, demonstrating that the debris was broadly terrestrial-like (Zuckerman et al. 2007). Since then, the broad pattern of bulk, Earth-like compositions has been seen – especially with ultraviolet *HST* observations – in several more stars

* E-mail: j.farihi@ucl.ac.uk

† STFC Ernest Rutherford Fellow

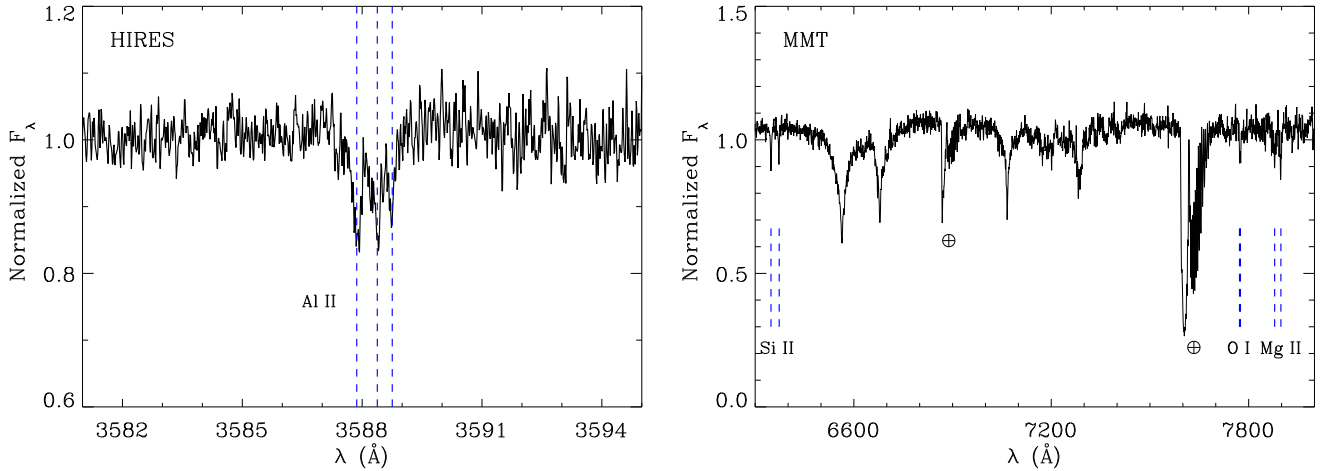


Figure 1. In the left panel is a portion of the HIRES spectrum, with wavelength given in vacuum and showing a strong triplet of Al II. The right panel shows a portion of the spectra obtained at the MMT, containing telluric features, H α , two He I, lines, and metal lines of O I, Mg II, and Si II. Unusually, the white dwarf exhibits strong lines of both H and He I, indicating a mixed atmospheric composition.

with five or more heavy elements (O, Mg, Si, Ca, Fe) that indicate melting and differentiation among extrasolar, rocky planetesimals, and a diversity of overall compositions similar to different classes of Solar System meteorites (Xu et al. 2013; Gänsicke et al. 2012).

Importantly, while most polluted white dwarfs appear to be contaminated by debris from parent bodies that were relatively poor in H₂O and other volatiles (Jura & Xu 2012), there is at least one case where substantial H₂O can be confirmed in an otherwise volatile- and carbon-poor planetesimal. The debris orbiting and polluting the atmosphere of GD 61 originated in a rocky minor planet roughly the size of Vesta and containing approximately 26% water by mass (Farihi et al. 2013b). Another polluted white dwarf with a substantial oxygen excess is SDSS J124231.07+522626.6, where the parent body likely had an even higher water content (Raddi et al. 2015). Such water-rich asteroids are important as potential building blocks of habitable planetary surfaces, especially if most small and rocky planets form dry as did the Earth (Morbiddelli et al. 2000).

This paper reports the identification and analysis of H, O, Mg, Al, Si, Ca, Ti, Cr, and Fe in the helium atmosphere white dwarf WD 1536+520. These elements are found to be accreting at a rate higher than any yet measured in a white dwarf with relatively short sinking timescales, and producing atmospheric metal abundances comparable to those of the Sun. The data are consistent with a refractory-rich parent body with a modest fraction of H₂O. Section 2 presents spectroscopic observations from several facilities that resulted in the detection of all the major rock forming elements, and strong upper limits on key volatiles. The atmospheric modeling is discussed in Section 3, along with the determination of stellar parameters, and elemental abundances within the star and the disrupted parent body. The paper explores the so-far unique properties of this star as something of a transition object between helium- and hydrogen-rich, polluted white dwarfs, with the conclusions presented in Section 4.

2 OBSERVATIONS

WD 1536+520 was first identified in the Second Byurakan Sky Survey (SBS 1536+520; Stepanian et al. 1999; Balayan 1997) in

1992 and correctly typed as a DBA (strongest lines He I, weaker lines of H) white dwarf from a low resolution, $R \approx 400$ spectrum. It was spectroscopically observed as part the Sloan Digital Sky Survey in 2002 (SDSS 153725.71+515126.9; Eisenstein et al. 2006), and exhibits lines of Mg, Si, and Ca in these $R \approx 2000$ data (Gänsicke et al. 2016), yielding a full spectral type of DBAZ. Given that the SDSS *ugriz* photometry alone results in a temperature estimate of 22 000 K (Girven et al. 2011), the presence of these metal absorption features in a modest resolution spectrum is remarkable – at similar T_{eff} and irrespective of atmospheric composition, the detection of atmospheric metals in white dwarfs typically requires powerful, high-resolution spectroscopy with Keck or the VLT (Koester et al. 2005). The star has an infrared excess detected by *WISE* (Debes et al. 2011b; Barber et al. 2014) at 3.4 and 4.6 μm , where the data are consistent with passively heated debris orbiting within the Roche limit, similar to roughly 40 other metal-enriched white dwarfs accreting from analogous disks (Farihi 2016).

Follow up observations were obtained in 2014 April with the MMT using the Blue Channel Spectrograph. Spectra were taken through a 1'' slit with the 8321 mm⁻¹ grating in first and second order, covering 6200–8100 Å at 2 Å resolution and 3200–4100 Å at 1 Å resolution respectively. The red spectrum consisted of four 900 s exposures in clear conditions, while the blue spectrum comprised three 600 s exposures but intruding on twilight where significant sky signal was present. The blue data are thus of relatively modest quality, while the red spectra are superior and a combined spectrum is shown in Figure 1. Most important, these modest resolution data exhibit a strong O I 7775 Å absorption feature, in addition to lines of Mg II, and Si II.

Additional, medium-resolution spectra were taken in 2014 July using the double arm ISIS spectrograph on the WHT. Simultaneous blue and red spectra were taken through a 1'' slit using the R1200B and R1200R gratings, with the 5300 Å dichroic, resulting in two spectra covering 4500–6000 Å at a resolution of roughly 1 Å. The white dwarf was observed continuously for eight exposures of 900 s in good conditions. The ISIS spectra reveal weak Al II and Si II features in wavelength regions not covered by the MMT dataset.

Lastly, high-resolution observations carried out in 2015 April with the HIREsb spectrograph on Keck I. The setup was identi-

Table 1. Stellar Parameters for WD 1536+520

SpT	DBAZ
g (AB mag)	17.06
d (pc)	217 ± 15
T_{eff} (K)	20800 ± 800
$\log g$ (cm s^{-2})	7.96 ± 0.10
Mass (M_{\odot})	0.58 ± 0.05
\log (H/He)	-1.7 ± 0.1
$\log (M_{\text{cvz}}/M)$	-11.16
Cooling Age (Myr)	62^{+16}_{-6}

Table 2. Lines Used for Abundance Determinations and Upper Limits

Ion	Vacuum Wavelength (\AA)
C II	4268
O I	7775
Mg II	4435, 4482
Mg I	5185
Al II	3588, 4664
Si II	3854, 3857, 3863, 4129, 4132, 5042, 5057, 6348, 6373
P II	3509, 3787
S II	4163, 5202, 5214, 5455
Ca II	3159, 3737, 3934
Ti II	3235, 3237, 3239, 3342, 3349, 3350, 3362, 3373, 3384, 3686, 3762
Cr II	3336, 3340, 3343, 3369, 3404, 3409
Fe II	3155, 3163, 3168, 3178, 3184, 3194, 3196, 3211, 3214, 3228, 3259, 3290, 3324, 3469, 3494, 5170, 5199, 5200, 5236, 5277, 5318

cal to that described in (Zuckerman et al. 2011), covering the range 3130–5940 \AA . The blue cross disperser was combined with a $1''$ 15 slit resulting in a spectral resolving power of $R \approx 40000$. Reduction procedures utilized both IRAF and MAKEE. This dataset reveals multiple lines of Mg II, Al II, Si II, Ca II, Ti II, Cr II, and Fe II, a portion of which is shown in Figure 1.

All spectra were reduced in the standard fashion, by average-combining each spectrum after extraction, using variance weighting for sky subtraction and rejection of bad pixels and cosmic rays.

3 ATMOSPHERIC PARAMETERS AND ABUNDANCE PATTERNS

The multiple spectral datasets were analyzed together using white dwarf atmospheric models, where the input physics is detailed in Koester (2010). The final stellar parameters were based on spectral fits to the latest SDSS spectrum, obtained with the BOSS spectrograph. We calculated a 3-dimensional model grid in T_{eff} , $\log g$, and [H/He], keeping the latter fixed while fitting the first two parameters. This is a more stable procedure than fitting for all three parameters, since the effect of [He/H] and $\log g$ on the spectrum is much smaller than that of the temperature. The results indicate the best fit is near 20800 K, which was confirmed by repeating a similar fit with $\log g$ kept fixed and fitting for T_{eff} and [H/He]. The final stellar parameters are given in Table 1.

For the determination of abundances and upper limits, all available spectra (Keck, MMT, SDSS, WHT) were used with the method of line profile fitting. Table 2 lists all the individual ions and wavelengths used for this purpose. After a good fit was approximated, models were re-calculated with ± 0.3 dex abundances,

Table 3. Abundances, Masses, and Accretion Rates for Trace Elements

Element	[Z/He]	[Z/He]	t_{diff} (yr)	Early Phase	Steady State
		$-$ [Z/H] $_{\odot}$		$X_Z M_{\text{cvz}}$ (10^{19} g)	\dot{M}_Z (10^9 g s^{-1})
H	-1.70		∞	4.012	
C	≤ -4.2		261	≤ 0.152	≤ 0.183
O	-3.40	-0.09	302	1.276	1.329
Mg	-4.06	+0.39	166	0.424	0.804
Al	-5.38	+0.16	141	0.023	0.050
Si	-4.32	+0.14	122	0.269	0.692
P	≤ -7.1		120	≤ 0.001	≤ 0.001
S	≤ -5.4		126	≤ 0.026	≤ 0.064
Ca	-5.28	+0.38	146	0.042	0.091
Ti	-6.84	+0.24	126	0.001	0.003
Cr	-5.93	+0.43	103	0.012	0.037
Fe	-4.50	+0.03	97	0.354	1.148
Σ				2.40	4.16

Note. Errors in abundance determinations are typically 0.1 – 0.2 dex. The fifth column is the mass of each element residing in the stellar convection zone, which consists of 8.0×10^{21} g of helium and 4.0×10^{19} g of hydrogen. Due to their continual sinking, the mass of heavy elements within the convection zone represents a minimum mass for the parent body. The metal-to-metal ratios within the planetary debris for the early phase and steady state regimes are derived directly from the values in the fifth and sixth columns respectively. The diffusion timescales are a sensitive function of T_{eff} within the range of acceptable temperatures for WD 1536, and thus contribute some additional uncertainty to the derived abundance ratios.

where visual inspection of each line determined the abundance and an error estimate. In the case of multiple lines the final abundance was determined as a weighted average. Repeating the analysis with T_{eff} and $\log g$ varied within the adopted errors, the systematic errors were found to be approximately 0.20 dex, but in the same direction for all elements. Relative abundance errors are 0.05 dex. The changes of the convection zone and diffusion timescales contribute 0.10 dex; and thus the total systematic error in relative abundances is 0.12 dex.

3.1 Bulk Composition of Accreted Debris

The abundances, relative to helium, of all trace elements are given Table 3, together with diffusion timescales for each species. The third column compares the atmospheric, heavy element abundances in the white dwarf (relative to He) in units of solar values (relative to H; Lodders 2003), demonstrating that WD 1536 nominally exceeds the solar values for nearly all detected elements. These absolute abundances surpass the previous record holder SDSS J073842.56+183509.6 (Dufour et al. 2010) by a factor of 3–10, and GD 362 by over an order of magnitude (Xu et al. 2013).

Also calculated are the mass of each element present in the photosphere of the star, which is equivalent to the mass fraction of a given element X_Z , multiplied by the mass of the convection zone M_{cvz} . If WD 1536 is in an early phase of accretion, where less than a single diffusion timescale has expired since the onset of atmospheric pollution, then the metal-to-metal abundances of the infalling debris are exactly mirrored by those in the atmosphere and given in the fifth column. If instead pollution has been ongoing for at least 5 diffusion timescales (Koester 2009), then the system is in a steady-state balance between accretion and diffusion and the abundance ratios are reflected in the sixth column. For all detected

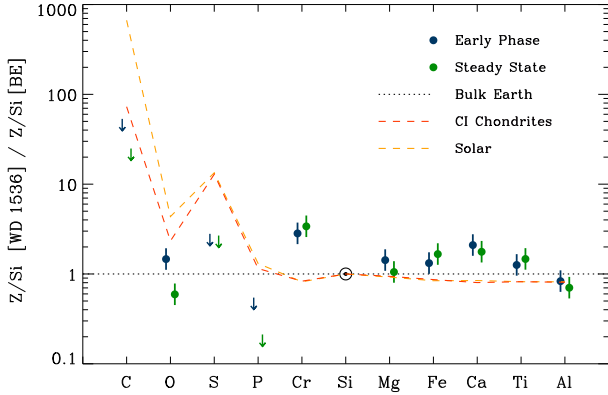


Figure 2. Derived number abundances for the planetary debris polluting the outer layers of WD 1536. Shown in blue and green respectively, are the early phase and steady state abundances of each heavy element relative to Si, divided by the same ratio as determined for the bulk Earth (Allègre et al. 2001). A typical uncertainty in the derived ratios is 0.12 dex, and error bars of this size are overplotted. Also plotted are the same ratios for CI chondrites and the Sun (Lodders 2003), demonstrating that these compositions can be confidently ruled out for WD 1536 based on ground-based data alone. At face value, the disrupted parent body appears broadly similar to the bulk Earth, with notably high chromium.

elements but oxygen, the metal-to-metal ratios show little variation between the early phase and steady state solutions.

In Figure 2 are plotted both the early phase and steady state abundances of heavy elements, relative to silicon and normalized to the bulk Earth values from Allègre et al. (2001). As can be seen, the debris orbiting and polluting WD 1536 is bulk Earth-like in the major rock forming elements to within a factor of around two. There is a notable enhancement in chromium, yet an apparent deficit in phosphorous. This two-fold deviation in opposite directions is difficult to reconcile, as both chromium and phosphorous are siderophiles with similar condensation temperatures (Lodders 2003). Similar enhancements in chromium have been seen in the white dwarfs PG 0843+516 and GALEX J193156.8+011745 (Gänsicke et al. 2012) – together with bulk Earth or higher phosphorous abundances, as expected – but are otherwise not commonly seen in polluted white dwarfs (Xu et al. 2014; Jura et al. 2012). Because phosphorous has only been detected in white dwarfs at ultraviolet wavelengths, the upper limit derived for WD 1536 from optical data may be uncertain. With this caveat, the data are consistent with the accretion of substantial core-like material.

3.2 Oxygen Excess and Hydrogen Accreted from H₂O

The total oxygen budget can be evaluated by accounting for all the expected oxides originating in planetary solids (Farihi et al. 2013b; Klein et al. 2010). In the early phase and steady state scenarios, oxygen is first assumed to be carried exclusively by MgO, Al₂O₃, SiO₂, CaO, and FeO within the debris. There are three possible outcomes from such an analysis.

(i) Insufficient oxygen to account for metal oxides. This outcome can imply that iron was delivered not as FeO but substantially as metal.

Table 4. Oxide, Iron Metal, and Water Mass Fractions

Oxygen Carrier	Early Phase	Steady State
MgO	0.22	0.40
Al ₂ O ₃	0.02	0.03
SiO ₂	0.24	0.59
CaO	0.01	0.03
FeO ^a	0.08	0.00
O Excess:	0.43	–
H ₂ O in debris:	0.25	–
Fe in metal:	0.00	1.00

^a Upper limit for FeO.

Note. The first five rows assumes oxygen is carried to maximum capacity by all the major rock forming elements, but in fact iron can also be in pure metal or iron-nickel alloy with no oxygen. The nominal oxygen budget in the steady state is unphysical unless 100% of the total iron is carried as metal, and the nominal O/Si and O/Mg ratios are marginally higher than tabulated.

(ii) An oxygen budget as expected for oxides in planetary solids. In this case the debris is rocky and poor both in water ices and hydrated minerals resulting from aqueous alteration.

(iii) Excess oxygen beyond that of anhydrous minerals alone. In this case, H₂O is the most likely source of the oxygen surplus.

Carbon can confidently be ignored as an oxygen carrier for the following reasons. First, carbon has been found to be significantly depleted relative to solar and volatile-rich, cometary abundance patterns in nearly all polluted white dwarfs where measurements are available (Wilson et al. 2016; Koester et al. 2014; Farihi et al. 2013a; Jura et al. 2012; Gänsicke et al. 2012; Jura 2006). Second, CO and CO₂ are no more than 5%–10% of the volatile content of Solar System comets, which are dominated by water ice (Binzel et al. 2000). Third, for WD 1536 in particular, the upper limit carbon abundance suggests that it cannot be a significant source of excess oxygen.

Table 4 evaluates the nominal oxygen budget for WD 1536 for both an early phase and steady state accretion history. In the steady state, there is insufficient oxygen to account for Mg, Al, Si, Ca, and Fe bound in oxides – *only if 100% of the iron was delivered as metal or alloy can the oxygen budget be considered balanced and physical*. In this case, the nominal oxygen abundance still requires a modest, 5 – 10% increase to account for the other elements (Mg, Al, Si, Ca) that only form rocks, but such leeway is well within the uncertainties. This is another strong indication that the material orbiting and polluting the white dwarf has a substantial core-like component. Of the total iron mass present in the Earth, metallic Fe in the core is thought to represent 87%, whereas Fe in the mantle and crust is only 13% (McDonough 2000), some of which is also metal. Thus, the scenario where the iron in WD 1536 was contained essentially in pure metals or alloys is plausible. Within the derived photospheric abundance errors, a steady state solution without any iron oxides would readily allow for solutions where the parent body contained water ice or hydrated minerals.

While the range of allowed abundance ratios also permits solutions without any excess oxygen, the striking hydrogen abundance in WD 1536 must be considered, and which clearly favors a water-rich interpretation. While an early phase of accretion predicts an oxygen excess and thus the need for H₂O within the planetary debris, the heavy element settling times are relatively short, and thus

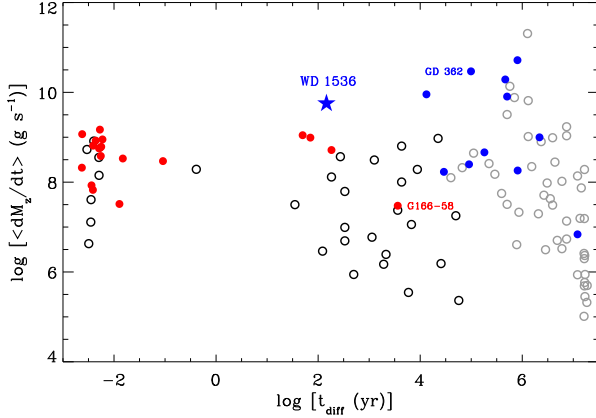


Figure 3. Accretion rate versus diffusion timescale for WD 1536 and a large sample of metal-enriched white dwarfs observed with *Spitzer* (Bergfors et al. 2014). For consistency, all plotted rates and timescales are based solely on Ca, following the method outlined in Farihi et al. (2012) with updated diffusion data (<http://www1.astrophysik.uni-kiel.de/~koester>; Koester 2009). The hydrogen-rich stars are shown as red filled and black open circles, while the helium-rich stars are shown as blue filled and grey open circles; filled symbols correspond to the detection of infrared excess. Within each atmospheric class, left to right represents decreasing T_{eff} . Remarkably, WD 1536 sits in a region that is otherwise exclusively occupied by stars with hydrogen atmospheres. G166-58 is the coolest white dwarf with a hydrogen-rich atmosphere and an infrared excess.

catching the star in this phase is less likely. If disks last for at least 10^5 yr (Girven et al. 2012), then the probability that WD 1536 is not yet in a steady-state phase of accretion is less than 1%. The total hydrogen mass within the stellar atmosphere is 4.0×10^{19} g, and could have been delivered by an asteroid with total mass a few to several times 10^{21} g and which was 5–10% H_2O by mass. This would be consistent with the lower mass limit of 4.2×10^{19} g from the heavy elements alone.

While uncertain, the totality of data discussed in this section favors the deposition of H_2O onto the stellar surface and carried by the parent body whose debris now orbits the star. In the next section, the anomalously high trace hydrogen abundance is shown to be transient, thus strengthening this interpretation.

3.3 Anomalous Diffusion Timescales and Trace H

The mass of the convection zone in WD 1536 is tiny – 10^6 times smaller than those within the bulk of known polluted white dwarfs with helium atmospheres. There are two reasons for this. First, the T_{eff} and 60 Myr cooling age mean the star is experiencing the early stages of convection zone growth (Paquette et al. 1986). In fact, with $T_{\text{eff}} > 20000$ K this star is the warmest and youngest helium-rich white dwarf to show metals due to ongoing accretion. Second, the anomalously high fraction of hydrogen leads to a significant reduction in the depth of the outer layers relative to a pure helium composition, by a factor of approximately 30.

These facts conspire to make the stellar atmosphere physically similar to a typical 10 000 K hydrogen-rich white dwarf, with comparable diffusion timescales. Figure 3 plots WD 1536 together with a sample of polluted white dwarfs observed with *Spitzer*, as a function of their inferred accretion rates and sinking timescales based on Ca II detections (Bergfors et al. 2014). WD 1536 lies above three hydrogen-rich stars whose disks have been detected in the in-

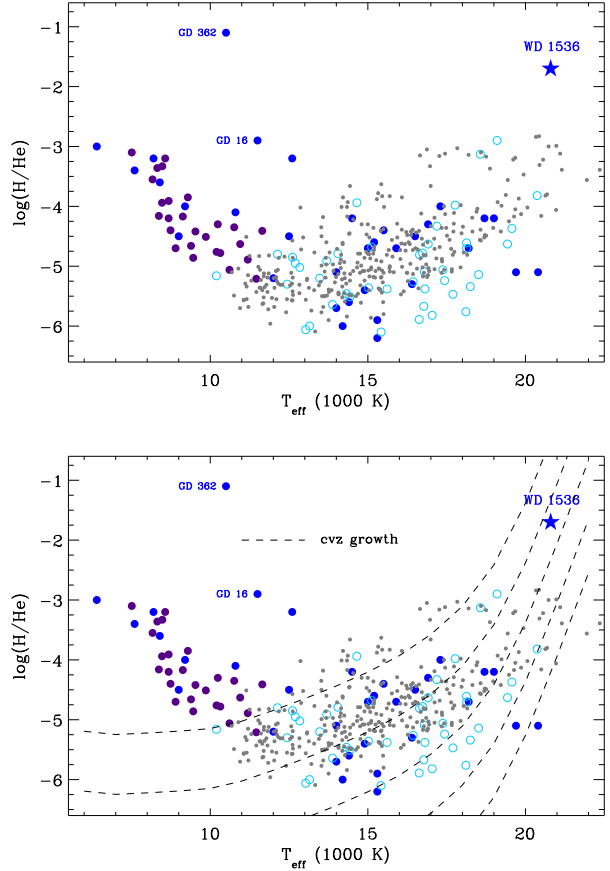


Figure 4. Relatively cool, helium atmosphere white dwarfs with detected hydrogen absorption. Light blue open circles are nearby stars from Bergeron et al. (2011) and Voss et al. (2007), while the grey dots are a more distant and abundant sample from Koester & Kepler (2015). Filled purple circles are stars with strong Ca II from Dufour et al. (2007), and filled dark blue circles are Figure 3 stars with matching criteria. The upper panel demonstrates the anomalous nature of WD 1536, whose H/He ratio is over an order of magnitude higher than any comparable object and second only to GD 362 (Zuckerman et al. 2007). Overplotted in the lower panel are tracks demonstrating the directly proportional change in H/He due to the growth of the convection zone over time in pure helium atmosphere stars (Koester 2009), shown for five orders of magnitude of initial $[\text{H}/\text{He}] = 1.0, 0, -1.0, -2.0, -3.0$. These calculations assume complete mixing of the outer layers.

frared (Farihi et al. 2010b; von Hippel et al. 2007), and has an even shorter sinking timescale than G166-58 (Farihi et al. 2008). This so-far unique position for a helium-dominated star strongly suggests 1) it is accreting at a high rate in a steady state, and 2) that the older, cooler stars with similar sinking timescales do not often experience similarly high rates of accretion. If this interpretation is correct, it would support a decreasing trend of planetary dynamical activity in the post-main sequence, as measured by the mass influx of planetesimals towards the white dwarf host, consistent with theoretical predictions (Mustill et al. 2014; Veras et al. 2013).

Figure 4 highlights the exceptional H/He in WD 1536. The upper panel plots samples of helium-rich white dwarfs with trace hydrogen detected directly through Balmer absorption features (typi-

cally only H α)¹. Interestingly, a substantial fraction of the plotted stars are also polluted with heavy elements, although a strong bias is present at $T_{\text{eff}} \lesssim 12000$ K. In this cooler temperature range, He I absorption rapidly becomes too weak to detect in low- and medium-resolution spectra, whereas strong Ca II absorption can indicate a helium-rich atmosphere (Dufour et al. 2007). At the warmer end of the temperatures shown in Figure 4, the bias towards metal detection is not an issue. Caution should be used when viewing Figure 4; the plotted stars do not represent an evolutionary sequence, and selection biases play a large role. That being said, the cooler stars with substantial hydrogen are either born with substantially more massive reservoirs than can currently be inferred in earlier evolutionary stages, or accrete H-rich planetary material.

3.4 H/He Evolution

Assuming complete mixing of the outer stellar layers, the lower panel of Fig 4 plots tracks of constant hydrogen mass within otherwise-pure helium atmosphere white dwarfs, as a function of temperature (Koester 2009). In this simple model where no stratification occurs between hydrogen and helium, the observational signature of most fixed masses of hydrogen at $T_{\text{eff}} \approx 20000$ K will gradually disappear from white dwarfs with helium-dominated atmospheres. The fact that some stars retain (or re-gain) substantial hydrogen masses at later times, is a well-known problem in white dwarf atmospheric evolution (MacDonald & Vennes 1991). While this general topic is beyond the scope of this paper, two distinct possibilities are 1) hydrogen is accreted over long timescales, or 2) primordial hydrogen floats over a deeper helium reservoir, and is later mixed into the photosphere. In the latter scenario, stars will appear hydrogen-rich at sufficiently warm temperatures and later reveal themselves to be helium-dominated (Bergeron et al. 2011; Fontaine & Wesemael 1987). Currently, there is more observational support for the primordial model, with at least 3/4 of helium atmosphere white dwarfs showing traces of hydrogen (Koester & Kepler 2015).

Thus in the absence of continued accretion WD 1536 will have both its metals and trace hydrogen wiped clean from its photosphere. Without the influence of ongoing, external pollution, the heavy elements will completely sink beneath the photosphere within a few 10^3 years at most. But over longer timescales, the remarkably high abundance of atmospheric hydrogen will be drowned by the deepening helium convection zone. By the time WD 1536 has cooled to 15 000 K in 140 Myr, the mass of the convection zone will have grown by 4 orders of magnitude and exhibit a trace hydrogen abundance $\log(\text{H}/\text{He}) = -5.7$. At this stage, the star will either appear as a fairly average helium-rich white dwarf, where hydrogen is difficult or impossible to detect in modest resolution spectra due to its apparent faintness relative to the nearby samples shown in Fig 4. When the star has cooled to 12 000 K after another 190 Myr, it will certainly not have detectable hydrogen. The unavoidable conclusion is that this white dwarf is being witnessed at a special time, in a transient phase, and the hydrogen is related to the orbiting planetary debris, and thus water is likely present.

Considering that WD 1536 may have only accreted $\sim 10^{19}$ g of hydrogen onto its atmosphere and $\log(\text{H}/\text{He}) = -1.7$, it can be seen that if a significantly larger and water-rich parent body

had been deposited, then hydrogen could (temporarily) have become the dominant atmospheric constituent. For example, the disrupted asteroids polluting GD 61 or SDSS 1242 might have delivered $\sim 10^{21}$ g or $\sim 10^{23}$ g of hydrogen respectively, resulting in abundances of $\log(\text{H}/\text{He}) \sim 0$ and $\log(\text{H}/\text{He}) \sim +2$. In both cases WD 1536 would temporarily appear as a hydrogen-rich star despite being dominated by the underlying helium. Therefore, the accretion of water-rich planetary debris has the potential to have an observable effect on H/He white dwarf spectral evolution.

4 CONCLUSION

The young, helium-atmosphere, white dwarf WD 1536 exhibits the highest abundances of heavy elements yet seen among polluted hosts of evolved planetary systems. In addition to the broadly solar abundances of the major rock forming elements O, Mg, Al, Si, Ca, and Fe, this star also has a remarkably high trace hydrogen abundance of $\log(\text{H}/\text{He}) = -1.7$. Considering the 1) abundance pattern of heavy elements, 2) the anomalously high trace hydrogen, and 3) the transient detectability of both the metals and the hydrogen, the most realistic conclusion is that the parent body whose debris is both orbiting and polluting WD 1536 contained traces of H_2O .

The thinness of the convection zone is a result of relative youth and relatively high mass of trace hydrogen within a helium-dominated atmosphere. Due to these combined facts, the outer layers of WD 1536 essentially behave as a hydrogen-rich white dwarf, with metal sinking timescales of only a few hundred years at most, hence supporting a steady state interpretation of the metal abundances. If these are indeed in a steady state, then WD 1536 has the highest *instantaneous* accretion rate yet observed among polluted white dwarfs.

ACKNOWLEDGMENTS

J. Farihi thanks S. Desch for feedback on a draft manuscript. The authors acknowledge both the MMT and WHT (Service program SW2014a39) for the expedient use of their Directors' time, without which these results would not have been possible, and an anonymous reviewer for feedback that improved the quality of the manuscript. J. Farihi gratefully acknowledges the support of the STFC via an Ernest Rutherford Fellowship. This research was supported in part by a NASA grant to UCLA, and by an NSF pre-doctoral fellowship to L. Vican. The research leading to these results has received funding from the ERC under the European Union's 7th Framework Programme n. 320964 (WDTracer).

REFERENCES

- Allègre C., Manhès G., Lewin É. 2001, *Earth Planetary Sci. Letters*, 185, 49
- Balayan S. K. 1997, *ApJ*, 40, 211
- Barber S. D., Kilic M., Brown W. R., Gianninas A. 2014, *ApJ*, 786, 77
- Bergeron P., Wesemael F., Dufour P., Beauchamp A., Hunter C., Saffer R. A., Gianninas A., Ruiz M. T., Limoges M. M., Dufour P., Fontaine G., Liebert J. 2011, *ApJ*, 737, 28
- Bergfors C., Farihi J., Dufour P., Rocchetto M. 2014, *MNRAS*, 444, 2147

¹ WD 1536 displays strong Balmer lines up to and including H δ .

- Binzel R. P., Hanner M. S., Steel D. I. 2000, in Allen's Astrophysical Quantities, ed. Cox, A. N. (4th ed.; New York: AIP Press; Springer), 315
- Bonsor A., Mustill A. J., Wyatt M. C. 2011, MNRAS, 414, 930
- Debes J. H., Hoard D. W., Wachter S., Leisawitz D. T., Cohen M. 2011b, ApJS, 197, 38
- Debes J. H., Sigurdsson S. 2002, ApJ, 572, 556
- Debes J. H., Walsh K., Stark C. 2012b, ApJ, 747, 148
- Dufour P., Bergeron P., Liebert J., Harris H. C., Knapp G. R., Anderson S. F., Hall P. B., Strauss M. A., Collinge M. J., Edwards M. C. 2007, ApJ, 663, 1291
- Dufour P., Kilic M., Fontaine G., Bergeron P., Lachapelle F. R., Kleinman S. J., Leggett S. K. 2010, ApJ, 719, 803
- Eisenstein D. J., et al. 2006, ApJS, 167, 40
- Farihi J. 2016, New Astronomy Reviews, 71, 9
- Farihi J., Barstow M. A., Redfield S., Dufour P., Hambly N. C. 2010a, MNRAS, 404, 2123
- Farihi J., Gänsicke B. T., Koester D. 2013a, MNRAS, 432, 1955
- Farihi J., Gänsicke B. T., Koester D. 2013b, Science, 342, 218
- Farihi J., Gänsicke B. T., Wyatt M. C., Girven J., Pringle J. E., King A. R. 2012, MNRAS, 424, 464
- Farihi J., Jura M., Lee J. E., Zuckerman B. 2010b, ApJ, 714, 1386
- Farihi J., Jura M., Zuckerman B. 2009, ApJ, 694, 805
- Farihi J., Zuckerman B., Becklin E. E. 2008a, ApJ, 674, 431
- Fontaine G., Wesemael F. 1987, in in IAU Colloq. 95, 2nd Conference on Faint Blue Stars, eds. A. G. D. Philip, D. S. Hayes, & J. Liebert (Schenectady: Davis), 319
- Frewen S. F. N., Hansen B. M. S. 2014, MNRAS, 439, 2442
- Gänsicke B. T., Farihi J., Koester D., et al. 2016, in preparation
- Gänsicke B. T., Koester D., Marsh T. R., Rebassa-Mansergas A., Southworth J. 2008, MNRAS, 391, L103
- Gänsicke B. T., Koester D., Farihi J., Girven J., Parsons S. G., Breedt E. 2012, MNRAS, 424, 333
- Gänsicke B. T., Marsh T. R., Southworth J., Rebassa-Mansergas A. 2006, Science, 314, 1908
- Gianninas A., Bergeron P., Ruiz M. T. 2011, ApJ, 743, 2011
- Girven J., Brinkworth C. S., Farihi J., Gänsicke B. T., Hoard D. W., Marsh T. R., Koester D. 2012, ApJ, 749, 154
- Girven J., Gänsicke B. T., Steeghs D., Koester D. 2011, MNRAS, 417, 1210
- Jura M. 2006, ApJ, 653, 613
- Jura M., Farihi J., Zuckerman B. 2007a, ApJ, 663, 1285
- Jura M., Farihi J., Zuckerman B. 2009a, AJ, 137, 3191
- Jura M., Xu S. 2012, AJ, 143, 6
- Jura M., Xu S., Klein B., Koester D., Zuckerman B. 2012, ApJ, 750, 69
- Jura M., Young E. D. 2014, AREPS, 42, 45
- Klein B., Jura M., Koester D., Zuckerman B., Melis C. 2010, ApJ, 709, 950
- Koester D. 2009, A&A, 498, 517
- Koester D. 2010, In Memorie della Societa Astronomica Italiana, 81, 921
- Koester D., Gänsicke B. T., Farihi J. 2014, A&A, 566, A34
- Koester D., Kepler S. O. 2015, A&A, 583, A86
- Koester D., Rollenhagen K., Napiwotzki R., Voss B., Christlieb N., Homeier D., Reimers D. 2005, A&A, 432, 1025
- Lodders K. 2003, ApJ, 591, 1220
- MacDonald J., Vennes S. 1991, ApJ, 371, 719
- McDonough W. F. 2000, in Teisseyre R., Majewski E., eds, Earthquake Thermodynamics and Phase Transformation in the Earth's Interior. Academic Press, San Diego, p.5
- Morbidelli A., Chambers J., Lunine J. I., Petit J. M., Robert F., Valsecchi G. B., Cyr K. E. 2000, M&PS, 35, 1309
- Mustill A. J., Veras D., Villaver E. 2014, MNRAS, 437, 1404
- Paquette C., Pelletier C., Fontaine G., Michaud G. 1986, ApJS, 61, 197
- Raddi R., Gänsicke B. T., Koester D., Farihi J., Hermes J. J., Scaringi S., Breedt E., Girven J. 2015, MNRAS, 450, 2083
- Rocchetto M., Farihi J., Gänsicke B. T., Bergfors C. 2015, MNRAS, 449, 574
- Stepanian J. A., Chavushyan V. H., Carrasco L., Tovmassian H. M., Erastova L. K. 1999, PASP, 111, 1099
- van Maanen A. 1917, PASP, 29, 258
- Vanderburg A., et al. 2015, Nature, 526, 546
- Veras D., Leinhardt Z. M., Eggl S., Gänsicke B. T. 2015, MNRAS, 451, 3453
- Veras D., Mustill A., Bonsor A., Wyatt M. C. 2013, MNRAS, 431, 1686
- von Hippel T., Kuchner M. J., Kilic M., Mullally F., Reach W. T. 2007, ApJ, 662, 544
- Voss B., Koester D., Napiwotzki R., Christlieb N., Reimers, D. 2007, A&A, 470, 1079
- Wesemael F. 1979, A&A, 72, 104
- Wilson D. J., Gänsicke B. T., Farihi J., Koester D., 2016, MNRAS, 459, 3282
- Xu S., Jura M., Klein B., Koester D., Zuckerman B. 2013, ApJ, 766, 132
- Xu S., Jura M., Koester D., Klein B., Zuckerman B. 2014, ApJ, 783, 79
- Zorotovic M., Schreiber M. R., Gänsicke B. T. 2011, A&A, 536, A42
- Zuckerman B. 2015, 19th European Workshop on White Dwarfs, ASP Conference Series 493 (San Francisco: ASP), 291
- Zuckerman B., Koester D., Melis C., Hansen B. M. S., Jura M. 2007, ApJ, 671, 872
- Zuckerman B., Koester D., Reid I. N., Hünsch M. 2003, ApJ, 596, 477
- Zuckerman B., Koester D., Dufour P., Melis C., Klein B., Jura M. 2011, ApJ, 739, 101